Science of the Total Environment 959 (2025) 178177

Contents lists available at ScienceDirect

Science of the Total Environment

journal homepage: www.elsevier.com/locate/scitotenv

Fine sediment-associated contaminants in gravel bed rivers: Evaluating storage times and turnover using fallout radionuclides (FRNs)

Enrique G. Muñoz-Arcos [a,*], Geoffrey E. Millward [a], Caroline C. Clason [b], Claudio M. Bravo-Linares [c], William H. Blake [a]

[a] School of Geography, Earth and Environmental Sciences, University of Plymouth, Plymouth PL4 8AA, United Kingdom
[b] Department of Geography, Durham University, Lower Mountjoy, South Road, Durham DH1 3LE, United Kingdom
[c] Instituto de Ciencias Químicas, Facultad de Ciencias, Universidad Austral de Chile, Independencia 631, Valdivia, Los Ríos, Chile

HIGHLIGHTS

- $^{7}Be/^{210}Pb_{ex}$ ratios reveal changes in dominant fine sediment sources after floods.
- Sediment storage times and turnover vary in response to floods.
- Sediment resuspension from in-channel storage is dominant during exceptional floods.
- Particulate trace metal concentrations on bars increase after exceptional floods.
- High recently deposited P in spring consistent with fertiliser application season.

GRAPHICAL ABSTRACT

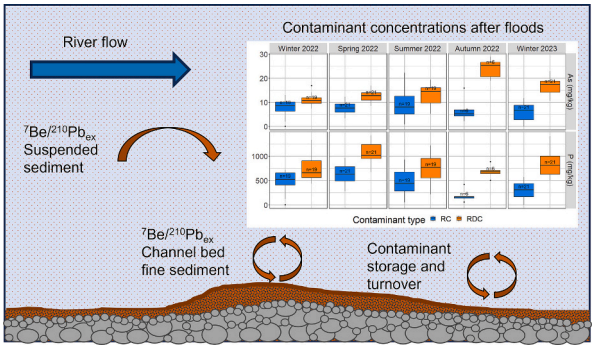

ARTICLE INFO

Editor: Bo Gao

Keywords:
Fine sediment
Radionuclides
Trace metals
Colmation
Clogging
Streambed
Nuclear and isotopic tools

ABSTRACT

Excess fine sediment supply and its associated contaminants can have detrimental effects on water quality and river ecology with sediment deposition on, and subsequent infiltration in, streambeds impacting riverine habitats. Fallout radionuclides (FRNs) are used as tracers in aquatic systems, and the $^{7}Be/^{210}Pb_{ex}$ ratio is a useful indicator for sediment residence/storage time. Suspended and submerged mid-channel bar sediments were collected during five surveys within a 5 km reach of a typical temperate lowland agricultural river system. Solids were analysed by gamma (^{7}Be and $^{210}Pb_{ex}$) and inductively coupled plasma (ICP, trace metals and phosphorus) spectrometry, and analysed for total nitrogen and organic carbon, to assess sediment dynamics and associated contaminant and nutrient storage. Significant spatial and temporal variation in $^{7}Be/^{210}Pb_{ex}$ activity ratios was observed, indicating changes in sediment sources closely related to contaminant inputs from legacy mining and agriculture. Storage times and the proportion of recently deposited sediment (RDS) varied between sampling sites and seasons in response to local channel characteristics and floods, which also influenced particulate contaminant distributions. This study demonstrates that FRN technology offers improved understanding of fine sediment and contaminant storage and turnover in river channel systems, which is vital to aid sediment management, river restoration and to tackle the global challenge of siltation and associated pollution in riverine habitats.

* Corresponding author.
E-mail address: enrique.munozarcos@plymouth.ac.uk (E.G. Muñoz-Arcos).

https://doi.org/10.1016/j.scitotenv.2024.178177
Received 7 August 2024; Received in revised form 14 October 2024; Accepted 16 December 2024
Available online 20 December 2024

1. Introduction

Excess fine sediment supply in river channels can have detrimental impacts on water quality and river ecology (Owens, 2020; Owens et al., 2005; Wharton et al., 2017; Wohl, 2015) as it acts as a vector for radionuclides (Millward and Blake, 2023), trace metals (Bravo-Linares et al., 2024), pesticides (Gellis et al., 2017), polycyclic aromatic hydrocarbons (Froger et al., 2019; Van Metre et al., 2022) and microplastics (Gerolin et al., 2020; Hurley et al., 2018), many of which have strong sorptive affinity with silts and clays (Bondarenko and Gan, 2004; Dong et al., 2013; Du Laing et al., 2009). Furthermore, sediment deposition on and subsequent infiltration in streambeds, a phenomenon also known as streambed colmation or clogging (Dubuis and De Cesare, 2023; Wharton et al., 2017), has been considered a pernicious problem because it impacts detrimentally on habitats for aquatic macrophytes, benthic invertebrates, diatoms and fish spawning gravels by reducing the hyporheic exchange and causing reduced pore water fluxes and oxygen supply (Bylak and Kukuła, 2022; Jones et al., 2012; Kemp et al., 2011; Wharton et al., 2017). Therefore, an improved understanding of fine particle dynamics and their associated contaminants in riverine ecosystems, specifically in channel beds, is critical to inform sediment remediation strategies and catchment-wide sediment management practices to tackle point and diffuse riverine pollution and supporting and regenerating aquatic biodiversity.

Storage of fine sediments in river corridors (i.e. channels and their adjacent floodplains) is a significant component of the fluvial sediment budget (Frings and Ten Brinke, 2018; Wohl, 2021) and it is associated with the often cited "sediment delivery problem" i.e. only a fraction of the total amount of sediment delivered to the channel exits the basin outlet (Fryirs, 2013; Walling, 1983). An expanding body of research has assessed the magnitudes (Collins and Walling, 2007; Marttila and Kløve, 2014), the controls (Evans and Wilcox, 2014; Gurnell and Bertoldi, 2022; Naden et al., 2016; Wilkes et al., 2019) and the impacts (Bylak and Kukuła, 2022; Pulley et al., 2019) of fine sediment storage in river channels. However, assessment of the associated time scales have received less attention due in part to the complexity of sediment dynamics in river channels and the lack of available methods (Muñoz-Arcos et al., 2022). Despite the difficulty of its evaluation, effective quantification of this component is essential when attempting to inform and predict the timescales for sediment management. For instance, if the temporal dynamics of sediment storage are better understood, then the timeframes when sediment management practices become effective can be better constrained.

Fallout radionuclides (FRNs) have been widely used as particle tracers in aquatic systems (Blake et al., 2002; Du et al., 2011; Kaste and Baskaran, 2011; Matisoff, 2014; Muñoz-Arcos et al., 2022) and can address this challenge. The basis for their use as tracers is their strong sorptive affinity with particles as shown by their high distribution coefficients, K_d, of the order of 10^4–10^5 L kg^{-1} (Hawley et al., 1986; Olsen et al., 1986; Van Hoof and Andren, 1989). However, their application as sediment residence/storage time tracers in rivers is limited (Muñoz-Arcos et al., 2022). Specifically, the $^{7}Be/^{210}Pb_{ex}$ ratio has been utilised as an indicator for sediment resuspension (Jweda et al., 2008; Olsen et al., 1989), transport distance (Bonniwell et al., 1999) and age/residence time (Gellis et al., 2017; Le Gall et al., 2017; Matisoff et al., 2005). Due to their different half-lives (^{7}Be $t_{1/2}$: 53.3 days and ^{210}Pb $t_{1/2}$: 22.3 years), ^{7}Be will decline rapidly compared to ^{210}Pb, thereby decreasing their ratio and reflecting the sediment age/residence time, hereafter referred to as the sediment storage time as specific riverine storage units are the focus of this article. The application of FRNs to assess sediment residence/storage times faces several challenges and research needs (Gellis et al., 2019; Le Gall et al., 2017; Muñoz-Arcos et al., 2022; Walling, 2013), particularly the effects of dilution of particulate ^{7}Be activity concentrations due to contributions from ^{7}Be-depleted sediment sources e.g. channel banks and/or resuspension from the channel (Walling, 2013). Moreover, the dynamics of sediment storage and the relationship with the occurrence of associated contaminants within river channels remains relatively unexplored (Muñoz-Arcos et al., 2022). The novel application of $^{7}Be/^{210}Pb_{ex}$ ratios taken in this work aims to address the research gaps identified above through the following specific objectives: 1) to estimate fine sediment storage times and the proportion of recently deposited sediment (RDSs) by exploiting differences in $^{7}Be/^{210}Pb_{ex}$ activity ratios between suspended and channel bed sediments (mid-channel bar surface sediments); 2) to assess the proportions of recently deposited contaminants (RDC) and residual contaminants (RC) after floods; and 3) to investigate relationships between sediment storage temporal dynamics and contaminant distributions in the river channel.

2. Material and methods

2.1. Study site

The River Avon (Devon, UK, Fig. 1) is a 40 km long gravel-bed river with a catchment area of 110 km^2. The mean annual flow is 3.7 m^3 s^{-1} and is moderated by management of the Avon reservoir in the upper catchment. Land use is characterised by rough hillslope and grazing areas in the upper catchment, whereas mixed arable and pasture lands dominate the middle and lower catchment. Sediment pollution dynamics in this catchment are influenced by anthropogenic activities. Metal mining activities, which produced relatively small amounts of ore, were carried out in the upper and middle catchment during the late 18th - early 19th centuries (Dines, 1956) with legacy arsenic (As), copper (Cu), lead (Pb) and tin (Sn) persisting in the river system (Wang et al., 2021). Currently, agriculture dominates in the middle and lower parts of the catchment, with increased phosphorus (P) concentrations since agricultural intensification post-1945 (Wang et al., 2021).

2.2. Sampling site selection and river monitoring

A 5 km river reach was used to evaluate sediment storage dynamics in the lower part of the Avon catchment. It is located above a monitoring station managed by the Environment Agency, UK, and the Normal Tidal Limit (NTL). Three well-established reported previously mid-channel bars (Muñoz-Arcos et al., 2024), located in the upper, middle and lower reach were selected as riverine geomorphological features of interest because they were subjected to changes in sediment composition/dynamics reflecting variations in streamflow, channel characteristics and sediment loads.

Water temperature, conductivity, turbidity and depth were continuously monitored using a calibrated Multi-Parameter TROLL 9500 sensor placed at the lower reach. In the upper reach the monitoring station was only used to record river level during selected storms and during the storm hydrograph sampling. The sensor was placed bankside, set to record readings at 15-min intervals, and was regularly maintained during monthly field visits. River discharge was obtained by means of a stage-discharge relationship. For this purpose, water velocity was recorded over a cross-sectional area of the river channel during four field surveys under various river flow conditions using an electromagnetic water velocity meter (model Fluvia – RC3). Water discharge was then computed by means of linear regression using river stage values as the predictor variable. Water samples were collected during one storm event to characterise time-dependant concentrations of suspended sediments in situ using an automatic water sampler (EBSCO) and turbidity was also recorded as nephelometric turbidity units (NTU). Water samples were filtered using pre-weighed filters (Whatmann GF/F glass fibre filters) that were carefully oven dried at 60 °C overnight, kept in a desiccator and finally reweighed. Suspended sediment concentrations (SSCs) were obtained by means of turbidity-SSC linear regression, and monthly suspended sediment loads (SSLs) subsequently computed as the sum of the products between discharge, SSC and time elapsed between readings.

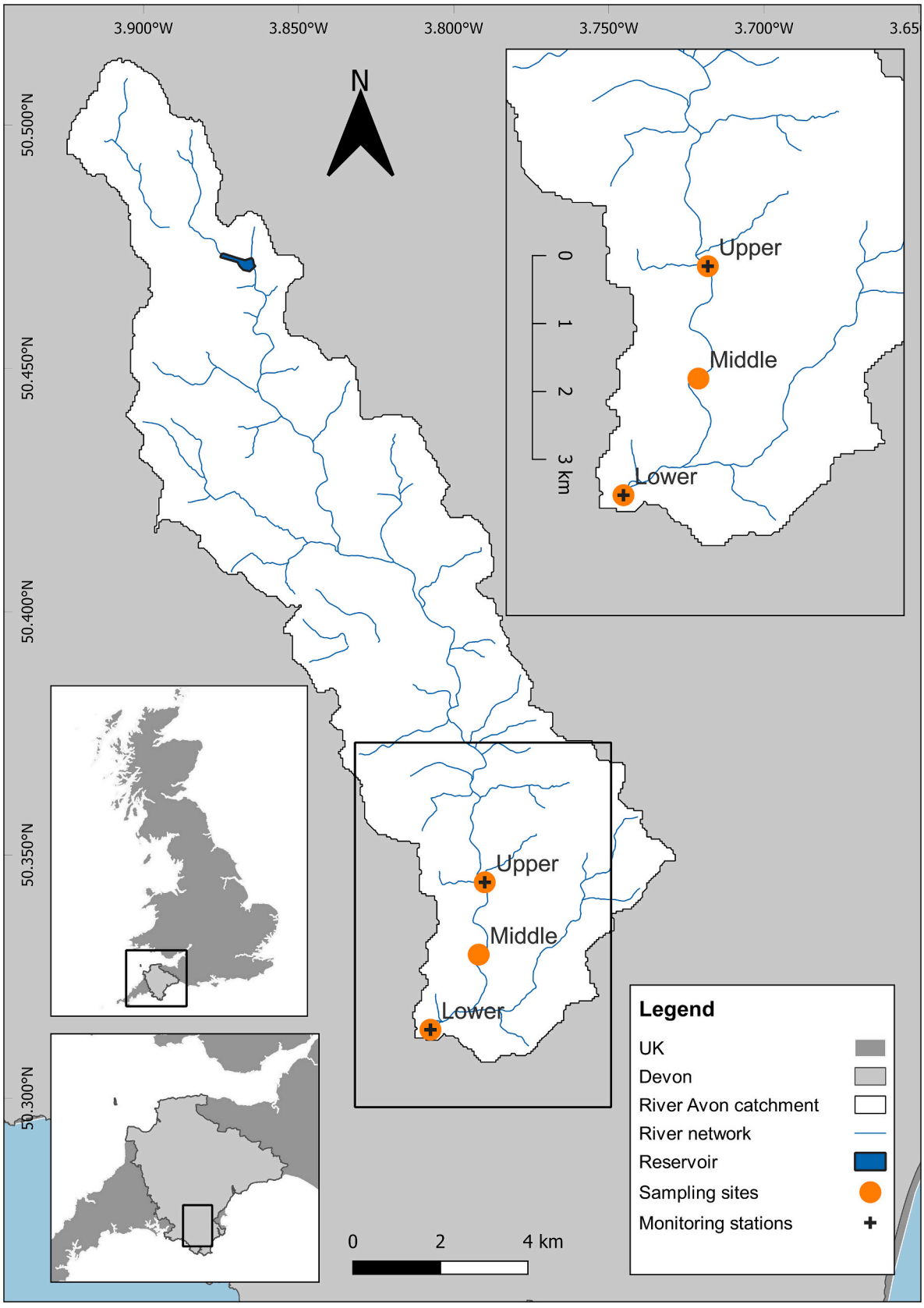

Fig. 1. Location of the River Avon catchment, south Devon, UK.

2.3. Sampling and sample preparation

Channel bar sediments (CBSs, $n = 106$) were sampled using the stilling-well resuspension method (Collins and Walling, 2007; Lambert and Walling, 1988). Briefly, a large plastic bottomless bin was placed on the riverbed to isolate the resuspendable sediments from the river flow and in three transects along the submerged mid-channel bars (i.e. head, middle and tail) to account for the spatial variability therein. Then, the bar surface was disturbed facilitating resuspension of fine particles. After resuspension, ~3 s of dwell time were allowed to let coarser grains settle before sampling the fine fraction. The suspended sediments were then collected using a plastic jar and quickly poured into acid rinsed 10 L HDPE containers. Water column height was recorded at each sampling point for estimation of sediment storage (see Supporting Information S1). The bars were sampled on five field surveys and after successive stormflow events. Suspended sediments (SSs, $n = 26$) were collected using time-integrated sediment traps (Phillips et al., 2000) placed at each sampling point (i.e. close to each channel bar). A detailed description of CBS and SS sampling can be found in Muñoz-Arcos et al. (2024). Samples were stored at 4 °C until further processing. Suspensions were allowed to settle overnight and dewatered, and the resultant sediment slurry was then centrifuged at 4000 RPM for 10 min and the supernatant discarded. Particles were subsequently freeze-dried until complete dryness was attained. Dried samples were disaggregated using a pestle and mortar and sieved across a clean stainless steel <63 μm sieve. Samples were packed in polyethylene bags for further analyses.

2.4. Sample analyses

2.4.1. Gamma spectrometry

Sediment samples were packed and sealed into aluminium containers, or 4 mL plastic vials in the case of low mass samples, and allowed to incubate for at least 21 days to promote the development of equilibrium between ^{222}Rn and its parent ^{226}Ra. Samples were counted for ~170,000 s using two calibrated HPGe gamma spectrometers (ORTEC planar detector model GMX50–83-LB-C-SMN-S and ORTEC well detector model GWL-170-15-S for low mass samples). ^{7}Be was determined from gamma emissions at 477 keV and ^{210}Pb$_{ex}$ was determined by subtraction of ^{226}Ra activity using ^{214}Pb gamma emissions (295 and 352 keV) from total ^{210}Pb (46.5 keV). Activity concentrations were decay-corrected to the sample collection date for CBS samples and to the date of the first flood for SS samples with high SSLs to correct for in situ decay of ^{7}Be inside the trap. Details about detector calibration, inter-detector comparison and quality control and assurance can be found in Muñoz-Arcos et al. (2024). Gamma counting was carried out at the ISO9001 certified Consolidated Radioisotope Facility at the University of Plymouth.

2.4.2. Particulate trace elements and phosphorus

All labware employed during weighing, filtration and dilution of the samples was placed in an acid bath (HNO_3 10 %) for 24 h, rinsed thoroughly with deionised water and subsequently with ultrapure Milli-Q water, then dried. Between 0.25 and 0.50 g of dried and sieved sediments were accurately weighed in 25 mL beakers for aqua-regia leaching following a modified aqua regia extraction procedure from ISO 11466:1995. Briefly, 1 mL of concentrated HNO_3 (analytical grade) was added to each sample, covered with a watch glass and digested on a cold hotplate for approximately one hour. Then, 6 mL of aqua regia mixture (HNO_3/HCl in a 1:3 ratio – both analytical grade) was added to each sample which was subsequently heated in stages until the contents were gently refluxing at approximately 95–105 °C. Leach solutions were refluxed for 2 h and until fumes were no longer evolving. After cooling to room temperature, samples were filtered and transferred quantitatively to 25 mL volumetric flasks and diluted with 2 % HNO_3. Procedural blanks were prepared in the same fashion as the samples and selected samples were leached in triplicate (i.e. repeatability, RSD < 10 %) together with a certified reference material (*Enviro*Mat – Contaminated Soil SS-2) for method validation of every digestion batch (ca every 35 samples). Furthermore, calibration curve verification was carried out before every run using a certified reference solution (*Enviro*Mat – Drinking Water, low EP-L, or *Enviro*Mat – Waste water, high EU-H) and instrument calibration checks were run every ten samples to confirm instrument stability (within ±10 % variation). Analysis of As was performed using an Inductively Coupled Plasma Mass Spectrometer (ICP-MS, Thermo Scientific iCAP TQ MS) whereas Cu, Pb, Sn and P were analysed using an Inductively Coupled Plasma Optical Emission Spectrometer (ICP-OES, Thermo Scientific iCAP 7400 ICP-OES). Elemental concentrations are reported in mg kg^{-1} of dry weight after correcting for potential moisture content acquired during sample storage (moisture content between 1 and 4 %). Quality control parameters are reported in the Supporting Information S2 (Table S2.1).

2.4.3. Total organic carbon (TOC) and total nitrogen (TN) in sediments

Total Organic Carbon analysis was carried out on subsamples varying from 0.1 to 1.0 g. Aliquots of diluted HCl (0.5 M) were added to the samples to ensure complete removal of carbonates. Approximately 20 mg of dried acid-treated (for TOC) and non-acid treated (for TN) samples were weighed into tin capsules and analysed using a CHN elemental analyser (Carlo Erba EA1110). Details about instrument calibration, blanks and quality control can be found in Muñoz-Arcos et al. (2024).

2.4.4. Particle size distribution

Subsamples (~ 1 g) of dried and sieved particles were treated with 2–3 mL of 6 % Hydrogen Peroxide (H_2O_2) and allowed to stand overnight. The samples were then placed in a water bath at 80 °C for 2 h and then removed and allowed to cool. The process was repeated to check for complete removal of organic matter. Sodium hexametaphosphate was added to every sample at a concentration of 0.1 % v/v to aid dispersion and avoid particle flocculation. Particle size distributions (PSD) were assessed using a Malvern Mastersizer-2000 laser diffraction particle size analyser. PSD results were statistically checked for large variability between replicates and a Relative Standard Deviation (RSD) of <5 % between selected percentiles (i.e. 5, 25, 50 -median, 75 and 95 percentiles) was defined as an acceptable result. The geometric specific surface area (SSA) was obtained from PSD data assuming that particles are both spherical and nonporous.

2.5. Estimates of storage times and RDS

Differences in ^{7}Be/^{210}Pb$_{ex}$ ratios between suspended sediments and surface deposits of the mid-channel bars at each site were used as an indicator of fine sediment storage times. Consequently, fine sediment storage time is defined as the time from when particles were transiting from the suspended load to when they are sampled in the channel bar at each site. Storage time, t, of sediments in the surface of the channel bars was computed using the Matisoff's equation (Matisoff et al., 2005):

$$t = \frac{-1}{\left(\lambda_{7_{Be}} - \lambda_{210_{Pb_{ex}}}\right)} ln\left(\frac{A}{B}\right) + \frac{1}{\left(\lambda_{7_{Be}} - \lambda_{210_{Pb_{ex}}}\right)} ln\left(\frac{A_0}{B_0}\right) \quad (1)$$

where A and B are the activity concentrations of ^{7}Be and ^{210}Pb$_{ex}$, respectively, in CBS samples, A_0 and B_0 are the activity concentrations of ^{7}Be and ^{210}Pb$_{ex}$, respectively, in SSs at each site (computed as mean activity ratios for each site), and $\lambda_{7_{Be}}$ and $\lambda_{210_{Pb}}$ are the decay constants for ^{7}Be and ^{210}Pb, respectively.

Estimation of sediment storage times was carried out under the following assumptions:

1) *Suspended sediment is the primary source of fine sediment deposited onto the surface of the channel bars*: Because channel bed deposits are in constant contact with the water column, it is reasonable to assume that they have been transported primarily as suspended load and

then deposited directly from suspension mainly during the falling limb of the storm hydrograph (Fisher et al., 2010; Lambert and Walling, 1988; Skalak and Pizzuto, 2010). Here, activity ratios from SSs are considered the 'source' activity ratios. Therefore, any changes in dominant suspended sediment sources, and consequently in activity ratios (e.g. from catchment surface to sub-surface, channel banks and/or resuspension) along the river reach are accounted for by sampling SSs proximate to each channel bar at each time.

2) *$^{7}Be/^{210}Pb_{ex}$ ratios in CBSs are not significantly influenced by changes in sediment properties or riverine conditions*: Because of similarities in their occurrence and distribution within river catchments i.e. both are primarily delivered from atmospheric fallout, positively charged and have high distribution coefficients, the $^{7}Be/^{210}Pb_{ex}$ ratio has been reported to correct for relative sorption and enrichment effects resulting from variations in grain size and particulate matter composition (Bonniwell et al., 1999; Matisoff et al., 2005).

The proportion of RDS (%) on channel bars was obtained as follows (Le Gall et al., 2017; Matisoff et al., 2005):

$$RDS\ (\%) = \frac{(A/B)}{(A_0/B_0)} \times 100 \quad (2)$$

In addition, the concentration of RDC (mg kg^{-1}) was estimated by:

$$RDC = \frac{RDS \times C_a}{100} \quad (3)$$

where C_a is the concentration of the a particulate contaminant.

The RC concentration (mg kg^{-1}) was further obtained as follows:

$$RC = C_a - RDC \quad (4)$$

2.6. Statistical analysis

Differences in $^{7}Be/^{210}Pb_{ex}$ ratios in both SS and CBS, and storage times and % RDS between seasons were assessed statistically. The Kruskal-Wallis rank sum test was performed on data grouped by seasons after failure to meet the normality assumption. Also, mean differences in storage times and % RDS were assessed statistically after surveys that were characterised by 'normal' high flow events (flow peak <15 m^3 s^{-1}) and exceptional floods (> 15 m^3 s^{-1}) using a two-sample t-test after checking for normality and homogeneity of variance assumptions. For this test, an outlier was removed after a Grubb's test (p-value <0.001), an interquartile range test and visual inspection. Differences between groups were considered statistically significant at the 95 % confidence level. Pearson's correlation analysis was carried out between activity ratios, SSA and TOC for CBS samples to test the assumption of $^{7}Be/^{210}Pb$ conservativeness. Relationships between particulate trace metals, P, TOC, TN and SSA were also evaluated using Person's correlation. Statistically significant correlations in both cases are reported at the 95 % confidence level.

3. Results and discussion

3.1. Fine sediment storage in response to floods

Mean fine sediment storage values per site were lowest in the upper reach in autumn 2022 (86 g m^{-2}), and the highest mean values were found in the middle reach bar in summer 2022 (496 g m^{-2}) reaching a maximum individual value of 1050 g m^{-2} (Table S1.2). Notably, sediment storage was higher in winter 2022 compared to both autumn 2022 and winter 2023 (Fig. 2d). Storage of fines, which can increase or decrease, was responsive to floods and depended on changes in streamflow and SSLs. For example, a consistent decrease in mean storage values per site was observed from winter to spring 2022 (Table S1.2), suggesting that after the floods between this period, fine sediment from river bars was released. The opposite is true from spring to summer, where river bars (except for the lower reach bar) showed high mean storage values (Table S1.2). This indicates that the streambed was replenished with fine sediment after the heavy rain event that occurred on 6th June 2022 which slightly increased streamflow but significantly increased SSC and consequently SSL (Fig. 2a, b and c). Similar dynamics were observed in autumn 2022 and winter 2023 (except for the middle reach bar). Therefore, fine sediment storage in the river channel is highly dependent on the frequency and magnitude of storms and flood events, which exert an oscillating release-replenishment pattern throughout the seasons (Fig. 2d).

3.2. Distribution of $^{7}Be/^{210}Pb_{ex}$ ratios

$^{7}Be/^{210}Pb$ ratios were consistently higher in SS samples compared to CBS samples throughout the seasons studied (Fig. 3). Seasonal median activity ratios were also statistically different in both SS and CBS samples (Kruskal-Wallis rank sum test, p-value <0.01). This suggests that there are additional environmental controls on seasonal activity ratios other than those attributable to random errors in sampling, sample processing and counting, which were carried out consistently throughout the study. Moreover, substantial spatial and seasonal variations in activity ratios were found in CBS samples. For instance, CBS activity ratios within sampling locations (i.e. bars) varied from 9 to 48 % and within seasons varied between 20 and 35 % (Table S3.1). The same is true for SS samples, where activity ratios varied seasonally from 12 to 30 % (Table S3.1). Therefore, activity ratios were found to vary significantly in time and space along the river reach in both SS and CBS samples.

The $^{7}Be/^{210}Pb_{ex}$ activity ratio has been used as indicator for sediment resuspension (Cornett et al., 1994; Jweda et al., 2008; Olsen et al., 1989). While $^{7}Be/^{210}Pb_{ex}$ ratios in SSs ranged from 2 to 3 in winter, spring and summer 2022, they decreased markedly to 1.5 after the autumn 2022 floods (Fig. 3), suggesting a switch in the dominant suspended sediment source, i.e. a source that was depleted in ^{7}Be while retaining $^{210}Pb_{ex}$ concentrations. We attribute this decline in activity ratios to significant fine sediment resuspension from the channel triggered by the autumn floods. This is supported by a decrease in fine sediment storage from summer 2022 to autumn 2023 (Fig. 2d). During summer months, particulate ^{7}Be activity concentrations in the channel bars had decreased significantly due to decay while $^{210}Pb_{ex}$ concentrations remained similar (Muñoz-Arcos et al., 2024). Another potential source to be considered are channel banks. However, it is well known that sediments from channel banks are depleted in FRN activity concentrations due to sheltering from fallout (Hancock et al., 2014; Walling and Woodward, 1992). A dominant contribution from channel banks would have decreased both radionuclides equally, causing no significant changes in their ratio in the SSs of autumn 2022. Caesium-137 distribution in CBS samples provides additional evidence in this regard. Had contributions from channel banks been significant, the activity concentrations of this radionuclide would have decreased markedly after the autumn floods but, in fact, it slightly increased (Muñoz-Arcos et al., 2024). Moreover, evidence of collapsing channel banks was not observed during this period and, in most of the reach, they were well-stabilised by riparian woodland that dominates this part of the catchment. This finding highlights the importance of considering the contribution of sediment resuspension from in-channel storage features to suspended sediment loads during extreme flood events in fine sediment tracing studies (Muñoz-Arcos et al., 2024).

Correlations between $^{7}Be/^{210}Pb_{ex}$ ratios and SSA in CBS samples was not significant through the seasons (R between −0.03 and 0.37, p-value >0.05. Fig. S4.1a), with a strong and significant association between $^{7}Be/^{210}Pb_{ex}$ ratios and TOC found in summer 2022 samples only (R = 0.78, p-value <0.001, Fig. S4.1b). The implications of the association between activity ratios and organic matter are discussed in Section 3.6.

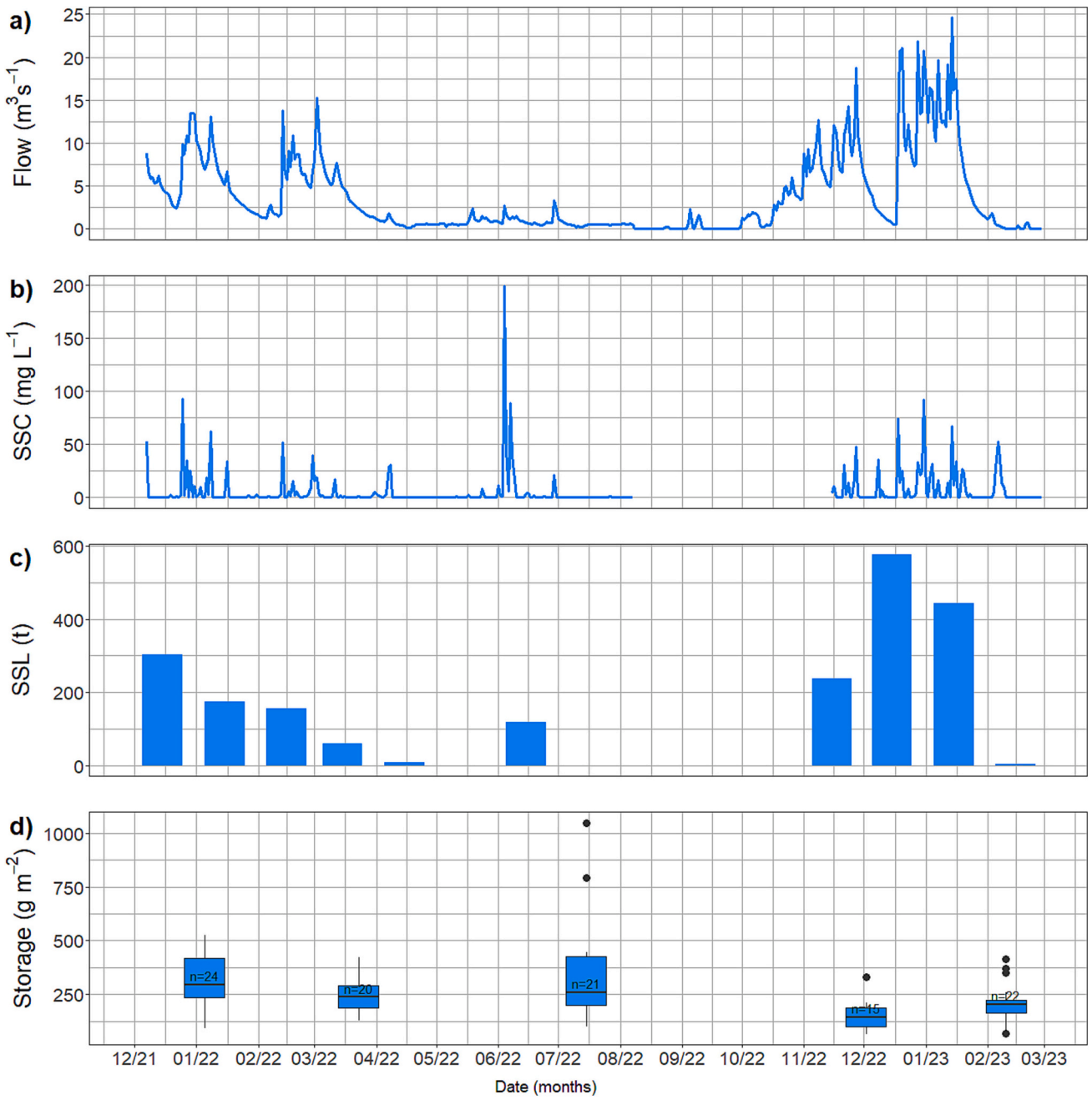

Fig. 2. River monitoring parameters at the outlet of the river reach and sediment storage distributions. a) Daily mean flow ($m^3 s^{-1}$); b) daily mean SSC (mg L^{-1}); c) monthly total SSLs (t); and d) sediment storage (g m^{-2}) distributions from the three sites at the time of sampling (x-axis) (for summary statistics see Table S1.2). Hereafter, boxes, horizontal lines, vertical lines and black dots in boxplots indicate interquartile range (25th to 75th percentiles), median, minimum and maximum and outliers, respectively. Note that SSCs and consequently monthly SSLs could not be estimated in September and October 2022 due to probe battery failure.

3.3. Storage times and proportion of RDS

Seasonal distributions (Fig. 4a) show that there are not only wide ranges of storage times in the river reach, such as the long and thin density function/violin plot in summer 2022, but also dominant storage times, as shown by the short and wide density plots in autumn 2022 and winter 2023. Storage times in the river reach were significantly different between seasons (Kruskal-Wallis rank sum test, p-value <0.01). Longer mean storage times were observed in the river reach in winter, spring and summer 2022 (44 ± 20, 37 ± 16 and 42 ± 31 d, respectively. Table S3.2), while substantially shorter mean storage times were observed after the autumn 2022 and winter 2023 floods (19 ± 14 and 26 ± 14 d, respectively). However, attention should be given to the spread of the distributions, highlighting the range of storage times dominating in the river reach which includes values from the three mid-channel bars. For example, storage times in summer 2022 show that the highest frequency of values is below 50 d, corresponding to the middle and lower reach sites. However, a small cluster of storage times can also be observed around 75 d during summer as noted by the data points in the grey violin plot (Fig. 4a), corresponding to the upper reach site. Interestingly, storage time values were higher in the upper reach site for most of sampling surveys, except in autumn 2022 and winter 2023 samples (Table S3.2). The highest proportions of RDS were found after the significant floods that occurred in autumn and winter 2022/23, whereas the lowest proportion obtained was in winter 2022 (Fig. 4b). Interestingly, in summer we find a wide range in the proportion of RDS (from 19

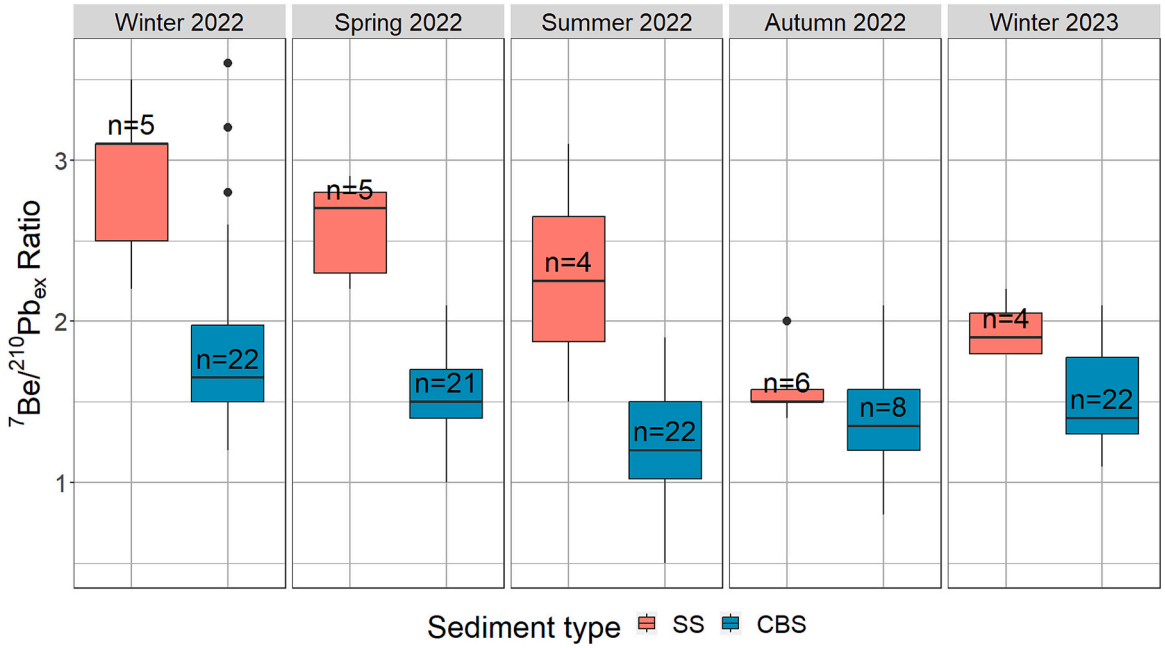

Fig. 3. Seasonal distributions of $^{7}Be/^{210}Pb_{ex}$ ratios in SS and CBS in the river reach.

to 96 %). Here, a lower mean proportion of RDS in the upper reach (34 ± 10 %) compared to means from the middle and lower reaches (77 ± 12 and 64 ± 17 %, respectively. Table S3.2) indicates that channel width and bar size exert significant controls on the deposition of fine sediment, which is discussed next. The median percentages of RDS between surveys were also statistically different (Kruskal-Wallis rank sum test, *p*-value <0.01).

Sediment storage times in surface channel bar gravels were responsive to flood magnitude. In general, two channel bar storage conditions can be ascribed here: 1) longer storage times with most values occurring between 25 and 75 d (Fig. 4a) were observed after floods that peaked below 15 $m^3\ s^{-1}$ (see flow in Fig. 2a), i.e. in winter, spring and summer 2022; and 2) shorter storage times with values < 50 d (Fig. 4a) were observed after floods that exceeded this river flow value i.e. in autumn 2022 and winter 2023 (Fig. 2a). Also, under the first storage condition, the proportion of RDS is relatively constant with interquartile ranges between 50 and 70 %, while a significant increase in RDS occurs in the second storage condition with interquartile ranges of between 80 and 90 % in autumn 2022 and between 60 and 90 % in winter 2023. The samples from these surveys were grouped as 'normal' and 'exceptional' events. Statistical analysis reveals that mean storage times and % RDS between these groups are significantly different (two-sample *t*-test, p-value <0.001). An explanation for these changes in storage conditions is that turnover of fine sediment on channel bars is dependent on the magnitude of floods. During 'normal' high flow events a limited amount of fine sediment is resuspended and immediately replenished from deposition during the falling limb of the storm hydrograph. When exceptionally high flow events occur, with a high potential for gravel bed mobilisation (Downs et al., 2016), removal of fine particles from the surface of the bars is almost complete, while limited replenishment takes place, as can be seen by the marked decreases in sediment storage values from summer to autumn 2022 and the winter 2023 surveys (Fig. 2d).

In addition, spatial differences in fine sediment storage along the river reach were also observed. High storage times and a lower proportion of RDS in the upper reach site in most of sampling surveys, except in autumn 2022 and winter 2023 (Table S3.2), can be attributed to channel bar size and local channel characteristics. In this site, the channel is narrower and the channel bar smaller compared to other sites (see measures in Table S1.1). These conditions make deposition of particles less efficient in the upper reach compared to the middle and lower reaches, where a wider channel and bigger bars allows a reduction in flow favouring deposition of recently delivered particles to the surface of the bars. During exceptionally high flows, as in autumn 2022 and winter 2023 (the second condition described above), this effect is less likely to occur. This can also be confirmed by sediment storage values, where the upper reach site has a consistently lower amount of sediment in storage across seasons (Table S1.2), highlighting the importance of channel characteristics on fine sediment storage dynamics, quantifiable using the methods presented in this study.

Comparison of channel bed storage times with those reported in the literature is not straightforward, as different methodologies have been employed and different particle size ranges targeted. Moreover, studies reporting channel bed storage/residence time using FRNs are scarce. For example, storage times of transitional bedload sediments (particle size between 0.063 and 2 mm) from submerged bars associated with in-channel obstructions (large woody debris and boulders) were estimated using ^{7}Be coupled with a constant initial activity (CIA) aging model (Fisher et al., 2010). Top core samples (0–5 cm) collected during summer (July–August 2006) in a 9 km reach of the Ducktrap River, central Maine, USA, exhibited storage times ranging from 'new' (indicating recent sediment deposition evidenced by negligible ^{7}Be decay from the mean CIA initial activity) to 85 days old. These storage times are comparable with those obtained during summer in this study (3–129 d, Table S3.2). Furthermore, channel bed deposits such as pools, channel margins, bars and glides were cored in summer 2009 in the White and West Rivers in east-central Vermont and the Mink Brook in New Hampshire, USA, and analysed for ^{7}Be and $^{210}Pb_{ex}$ (< 2 mm particle size) to model bed sediment residence time using a stacked reservoir model (Gartner et al., 2012). Under conditions with complete downward mixing of infiltrating particles, residence times in the 5 to 10 cm core sections (comparison with the top core section could not be done since residence time is not calculated for the 0–5 cm core section in this model), ranged from 3 to 7 d. Under the no mixing scenario, residence times in the same core sections ranged from 15 to 37 d.

The application of the $^{7}Be/^{210}Pb_{ex}$ ratio as a chronometer for estimating sediment residence/storage time in rivers has, however, been subject to criticism (Walling, 2013). For instance, the use of a constant value for the initial activity ratio, and the assumption that freshly

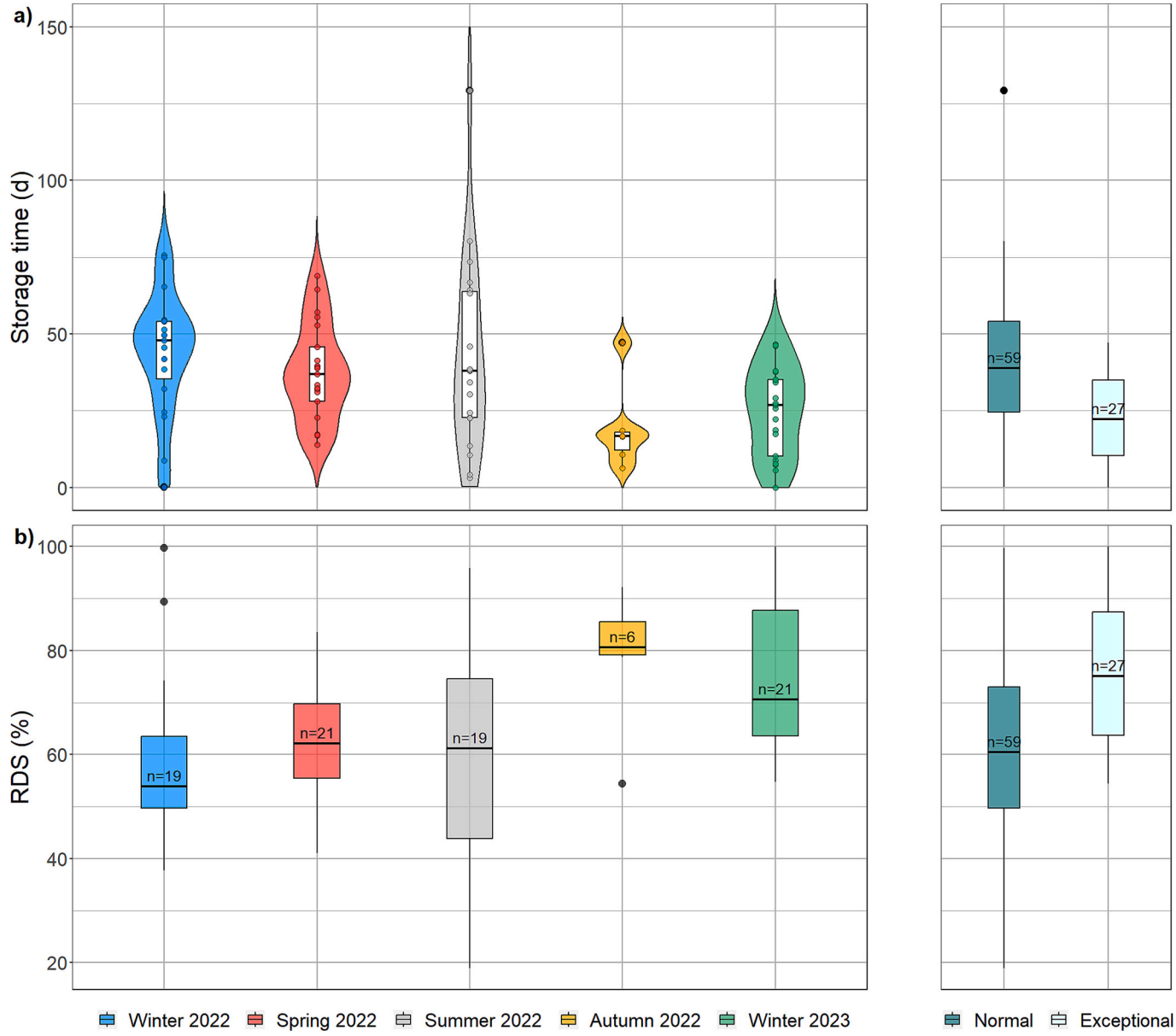

Fig. 4. Distribution of a) storage times (d) and b) proportion of RDS (%) grouped by seasons (left panel) and flood magnitude defined as peak flow below (normal, winter spring and summer 2022) and above (exceptional, autumn 2022 and winter 2023) 15 $m^3 s^{-1}$ (right panel). Density (violin) plot area is scaled to reflect sample size and boxplots and point values are superimposed to observe clusters of storage times. Note that every survey includes values from the upper, middle and lower reach sampling sites.

mobilised sediment could be characterised by an activity ratio similar to that of rain (Walling, 2013). However, these assumptions are not supported in the current literature due to significant spatial and temporal variations in rain activity ratios (Gourdin et al., 2014) and sediment source controls on activity ratios during early stages of sediment mobilisation and delivery (Walling, 2013). Activity ratios from ephemeral flows in catchments where sediments are mostly derived from the surface emerged as an opportunity to better characterise initial activity ratios, as these ratios would readily acquire the signature from their dominant sediment sources (Le Gall et al., 2017). However, this approach does not consider potential signal dilution with contributions of ^{7}Be-depleted sediment by resuspension, due to in-channel storage and decay, to the suspended load. In the present study, targeting fine sediments on channel bed deposits and sampling suspended sediments at each site allowed not only the characterisation of activity ratio variation due to potential changes in dominant sediment sources, both spatially and temporally, along the river reach, but also assessment of sediment storage times and turnover in local channel deposition areas. This is of relevance for channel ecology and river restoration assessments as these channel zones provide habitats for aquatic insects and salmonids spawning gravels.

3.4. Distribution of particulate trace metals, phosphorus, TOC and TN in channel sediments

Distribution trends of sediment-associated contaminants and nutrients in SS and CBS samples are closely related, and most of these elements varied significantly between seasons (Fig. 5). For instance, the highest concentrations of As and Pb were found in autumn 2022 and winter 2023 in both SS and CBS samples. On the other hand, Sn concentrations were higher in winter 2023 in SSs and in autumn 2022 in CBSs. Cu concentrations in SSs were highest in spring 2022, while concentrations in CBSs were high in both winter periods. P concentrations were high in spring in both SS and CBS samples. Organic

constituent concentrations (TOC and TN) were higher in summer 2022 CBS samples and in autumn 2022 SS samples. The lowest concentrations in both SSs and CBSs occurred in summer 2022 for Cu, Pb and Sn and in winter 2022 for As. P, TOC and TN concentrations were lower in autumn 2022 and winter 2023 for CBS samples. Notably, elements such as Cu, Pb, Sn and P showed a significant decrease in concentrations in both SS and CBS samples from spring to summer 2022. As, Cu, Pb and Sn showed a substantial increase in concentrations from summer to autumn 2022 in CBS samples, while P, TOC and TN showed the opposite behaviour.

Statistically significant ($p < 0.01$) and strong positive correlations were found between As, Cu, Pb and Sn in CSB samples (Fig. 6), and these elements were negatively correlated with TOC, TN and P (except Cu). Particulate phosphorus, on the other hand, showed positive and significant correlation with TOC, TN, SSA and Cu ($p < 0.01$, Fig. 6). Moreover, SSA showed a strong positive and statistically significant correlation with Cu and P, and negative relationship with Sn.

Low concentrations of particulate trace metals in CBS samples occurred during summer 2022, whereas high concentrations occurred in autumn 2022 and winter 2023. In addition, high P concentrations occurred in spring but lower concentrations in autumn 2022. These fluctuations can be attributed to changes in dominant suspended sediment sources contributing to the channel bars. While P, TOC and TN are generally associated with catchment erosional inputs from agriculture, trace metals such as As, Cu, Pb and Sn are associated with the natural underlying geology and legacy mining in this catchment (Dines, 1956; Wang et al., 2021). The inverse relationship between these metals and P, TOC and TN (Fig. 6) suggests that their occurrence in the fine sediment deposits on the channel bars is mainly controlled by changes between these two sources. In this case, natural and legacy trace metals that are already present in the river system are reworked/resuspended during extremely high flow events, increasing their concentration within the aquatic habitat up to 2-fold in both suspended and channel bed

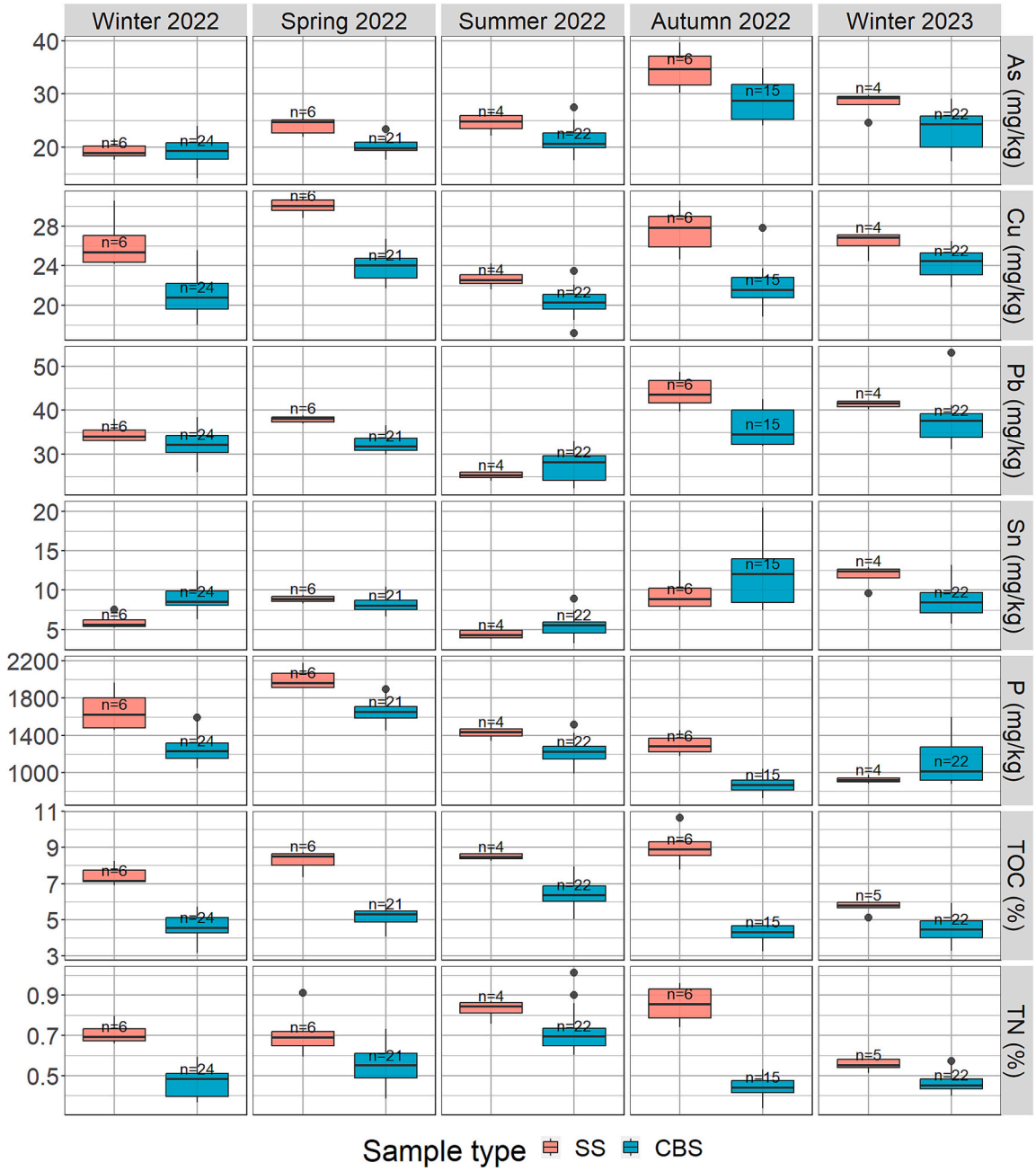

Fig. 5. Seasonal distribution of selected particulate trace elements and phosphorus (mg kg^{-1}), and TOC and TN (%) in SS and CBS samples.

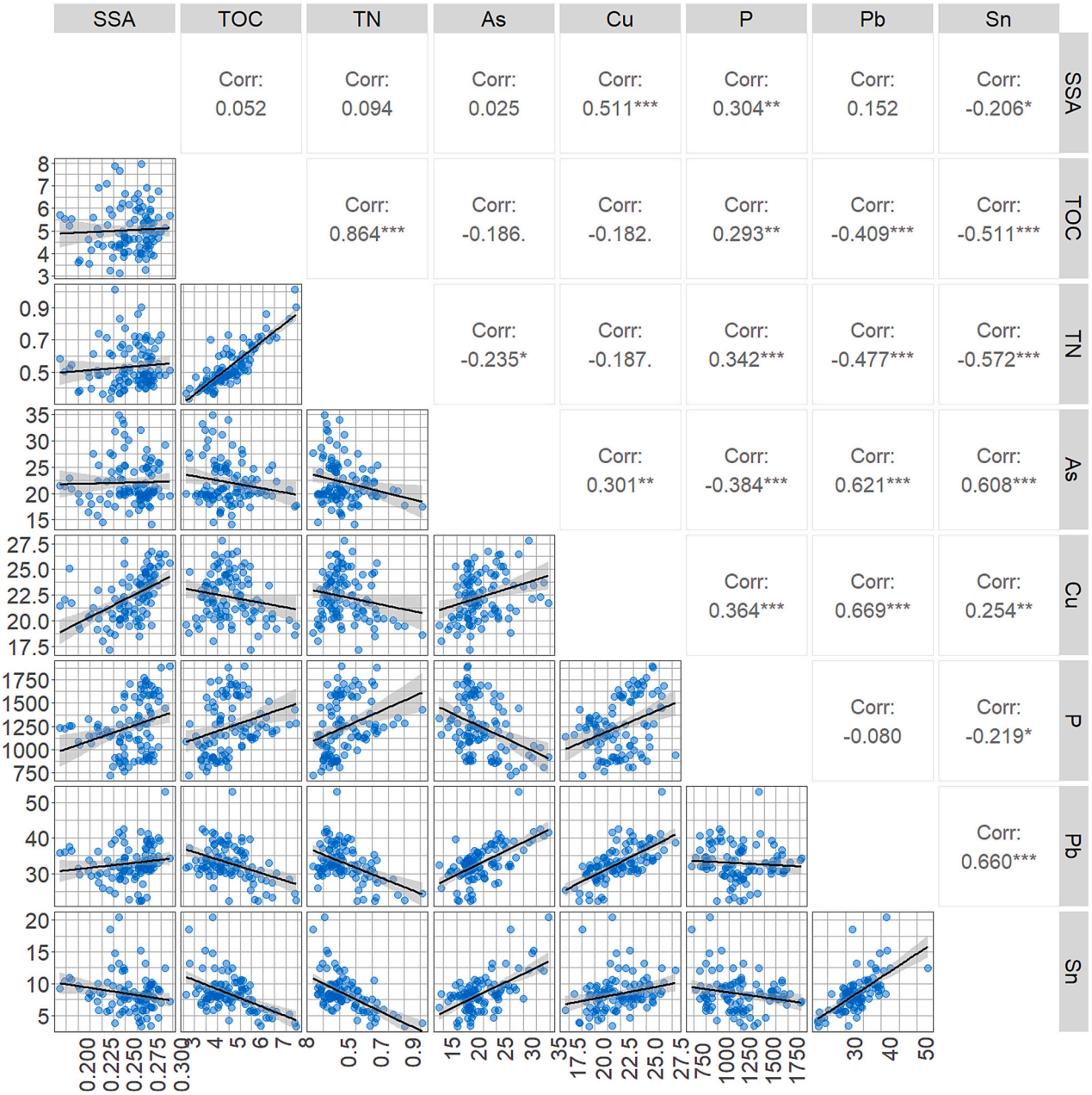

Fig. 6. Correlation matrix between TOC, TN (%), SSA ($m^2\ g^{-1}$) and selected particulate trace metals and phosphorus (in mg kg^{-1}) in CBS samples (*: *p*-value ≤0.05; **: p-value ≤0.01; and ***: p-value ≤0.001).

sediments.

3.5. Distribution of RCs and RDCs

The RDC concentrations of particulate trace metals, TOC and TN in the channel bars slightly increase between winter to spring 2022 samples, with P increasing significantly during this period (Fig. 7). During summer 2022, RDC concentrations slightly decrease for the metals while TOC and TN increase. During this period RC concentrations are variable, but a consistent decrease towards summer 2022 is apparent for most elements, except for TOC and TN (Fig. 7). After the floods of autumn 2022, RC concentrations declined significantly while RDC concentrations increased 3- to 4-fold for all elements (Fig. 7). Differences between RC and RDC concentrations were maximised during this period. Of note, after these floods, particulate trace metals reached their highest concentrations in the channel bars, except for Cu, P, TOC and TN (Fig. 5). In winter 2023, RC concentrations slightly increase while RDC concentrations decrease for all elements. RDC concentrations remain high during this period while RC concentrations remain relatively low compared to winter, spring and summer 2022 surveys (with the exception of P, TOC and TN), highlighting the influence of the magnitude of floods on the distribution of fine particulate contaminants on the channel bed. The RDC estimations for CBS samples confirmed that most of the particulate trace metals in CBS samples were recently delivered during the autumn 2022 and winter 2023 flood events. The decline in $^{7}Be/^{210}Pb$ ratios during this period suggests a dominant contribution of particulate trace metals from resuspension of in-channel fine sediment deposits. This finding highlights the significance of in-channel short-term storage deposits as a secondary source of particulate contaminants during extreme floods. In addition, high RDC concentrations for P in spring 2022 samples are attributed to the dominant erosion inputs from the catchment, with most of the particulate P being recently delivered to

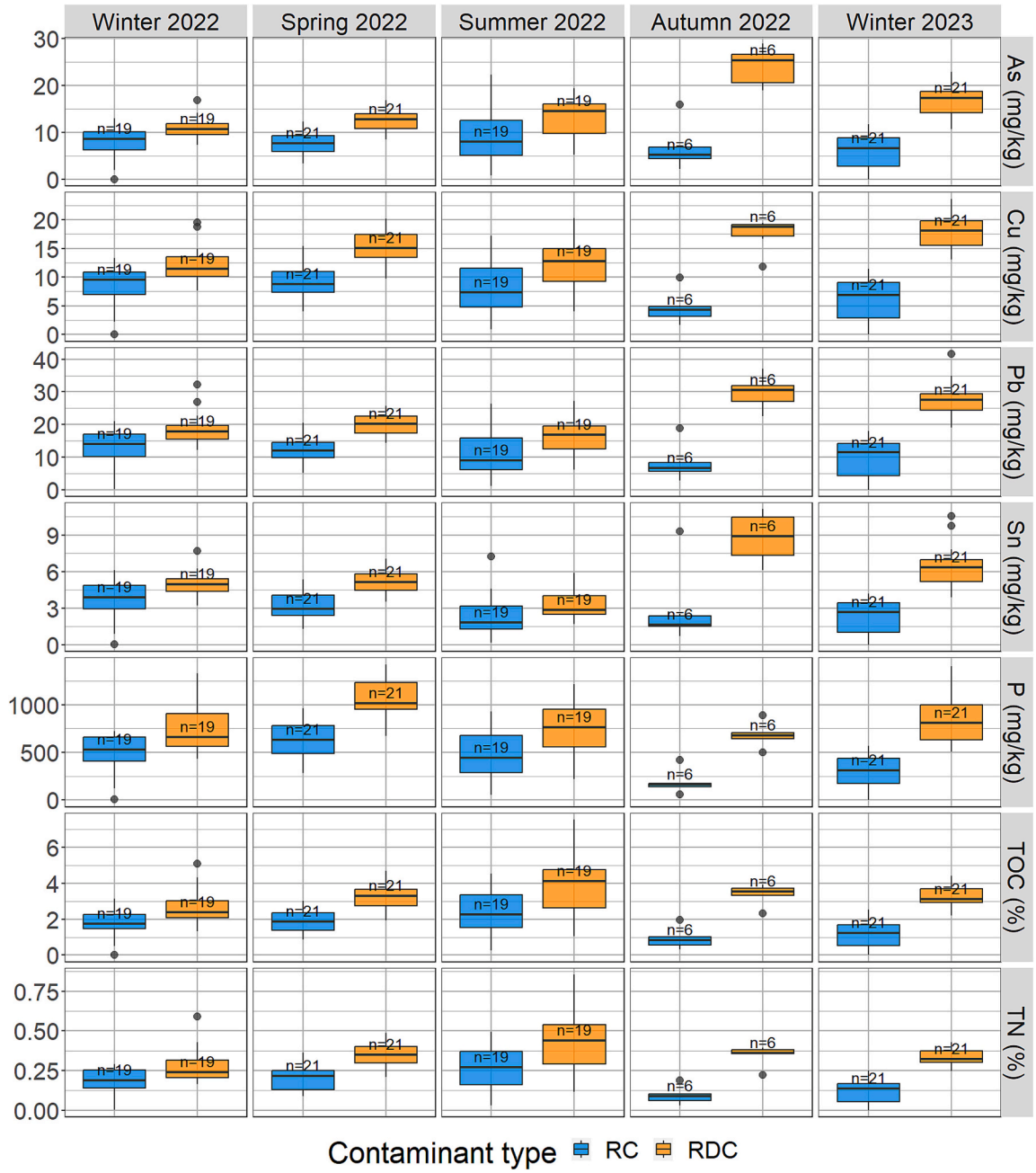

Fig. 7. Seasonal distribution of selected RCs and RDCs in CBS samples.

the channel. This was anticipated, as spring is also the season when phosphate fertilisers are applied to crops and fields and can be washed off during rain events, contributing a substantial amount of particulate P to streams. Moreover, moderate although statistically significant correlations between P and TOC and TN (Fig. 6) suggests that their occurrence in fine channel bar sediments was controlled by the same process(es) i.e. erosion inputs from the catchment. Hence, their RC and RDC trends are expected to be similar.

3.6. Methodological considerations for global applicability

Although the application of $^{7}Be/^{210}Pb_{ex}$ ratios as a tracer for storage times and proportion of RDS provided significant information on sediment storage dynamics, its application is not straightforward. Some of the challenges that should be considered in future studies are described below.

Penetration depth during the resuspension of the channel bed can be a source of variability, particularly for ^{7}Be, as it cannot be precisely controlled. Although the sampling program was carried out consistently and carefully to only disturb the fines stored on the surface of the bars, we observed that ^{7}Be concentrations in CBS samples from all surveys were subject to higher variation (coefficient of variation = 32 %) compared to $^{210}Pb_{ex}$ (coefficient of variation = 22 %), suggesting that the resuspension method might have influenced ^{7}Be variability over and above the random variation from sample processing and analysis. Recovering fine particles from gravel bed rivers can be difficult, as using a coring method such as freeze coring adds complexity to the logistics and the possibility of characterising as much spatial variation in sediment storage within and between channel deposits as possible, let alone the amount of fine material available for radiometric analysis.

Characterisation of initial $^{7}Be/^{210}Pb_{ex}$ ratios can also be a challenge. We used time-integrated sediment traps (Phillips et al., 2000) to sample

suspended sediments during floods. This sampling method integrated variations in activity ratios within and between successive storms during the studied periods. However, activity concentrations of ^{7}Be and $^{210}Pb_{ex}$ have been reported to vary during the storm hydrograph (Blake et al., 2002; Evrard et al., 2016; Muñoz-Arcos et al., 2024). For example, activity ratios from samples collected during one minor storm event in November 2022 in the upper river reach varied by 16 % (Fig. S5.1). Therefore, implementing sampling devices which are able to capture settling particles, especially during the falling limb of the storm hydrograph, would further improve the technique by accurate characterisation of the depositional (source) activity ratio.

River channels are highly dynamic. Here, we targeted mid-channel bars as these features were found consistently along the river reach under investigation. However, we found substantial spatial variation in activity ratios related to channel width and bar size. We infer that channel forms such as pools and riffles, lateral deposits and point bars would also show substantial spatial and temporal variation amongst them at a reach- and river-scale. As discussed in Section 3.2, variation imposed by changes in sediment sources is also important. Significant effort was made to characterise variation within bars, between bars and seasonally. However, characterisation of the variability between different channel forms and inter-annual variations in sediment loads, and changes in dominant sediment sources, require a detailed channel sampling approach along reaches and over several years of continuous survey, respectively. Therefore, we recognise that these sources of variability are not quantified within the timeframe and objectives of our sampling design, but it opens avenues for future research.

The use of $^{7}Be/^{210}Pb_{ex}$, rather than ^{7}Be or ^{210}Pb alone for example, has been reported to correct for relative sorption and enrichment effects resulting from variations in grain size and particulate matter composition (Bonniwell et al., 1999; Matisoff et al., 2005). However, we found a significant correlation between activity ratios and TOC in summer CBS samples (Fig. S4.1). This association is mainly driven by increasing ^{7}Be activity concentrations with increasing TOC (Muñoz-Arcos et al., 2024). Typically, during dry seasons with low rainfall and reduced river flow, a lacustrine-like condition may be induced where an increase of water temperature favours algae growth and autochthonous organic matter production (Lee et al., 2019). Under this scenario, scavenging of ^{7}Be onto particles is efficient as it is delivered as Be^{2+} which is highly competitive for cation exchange sites and thus highly particle reactive (Kaste et al., 2002), especially if small storm events do not generate significant sediment loads and direct channel precipitation is considerable (Karwan et al., 2018; Kaste et al., 2014). Therefore, the $^{7}Be/^{210}Pb_{ex}$ ratio conservativeness during long periods of storage and changing riverine conditions should be carefully examined. Enrichment of ^{7}Be due to enhanced scavenging by organic matter is likely to have influenced sediment storage time and RDS estimations in summer 2022 samples, with values possibly being underestimated and overestimated, respectively.

3.7. Implications for tackling the global aquatic siltation and contamination challenge

Dynamics of fine sediment and associated contaminant storage have critical implications for river channel ecology (Bylak and Kukuła, 2022; Naden et al., 2016; Wharton et al., 2017; Wilkes et al., 2019; Wohl, 2015). Here we show how coupling FRNs with contaminant assessment can support critical decision making in tackling the fine sediment siltation and contamination challenge. Furthermore, this work demonstrates the complexity of assessing in-channel sediment-associated contaminants and the need for in-depth consideration of siltation processes when assessing pollution status of aquatic habitats. Fine sediment storage times and activity ratios can be associated with channel habitat quality for macroinvertebrate communities, as filter feeders, for example, benefit from stable and low fine sediment storage substrates with rapid sediment and nutrient turnover (Svendsen et al., 2009). Elevated storage of fines along with increased residence times have the potential to detrimentally impact channel bed habitats by clogging interstitial pore spaces, reducing hyporheic and nutrient exchanges. Fine sediment-associated contaminants in the channel bed also have the potential to become bioavailable with longer storage times and under changing riverine conditions, such as pH, redox and organic matter composition, negatively impacting biota and river water quality. Also, enrichment by nutrients such as P and N in river sediments can lead to eutrophication. Improved understanding of channel storage dynamics of fine sediment and associated contaminants is therefore crucial to inform catchment sediment management practices. Climate change, and thus changing rainfall patterns and occurrence of floods, will present a major challenge for sediment management. This research highlights that it is not only erosion from the catchment that can contribute to increased particulate contaminant loads in both suspended and channel bed sediments, but also resuspension of legacy contaminants from short-term channel storage deposits during and after extreme floods. The reach selected in the River Avon presented an exemplar natural laboratory where dynamics of sediment storage in the channel were responsive to events at a catchment scale. Consequently, improved pollution control measures are necessary, and some recommendations can be made. For example, alleviating soil compaction to prevent surface run-off and erosion, and improved barriers such as buffer strips to reduce diffuse pollution from agriculture. With regards to legacy particulate trace metal occurrence in the channel, implementation of natural flood management techniques provides an opportunity to attenuate fine sediment and associated trace metal resuspension. Estimation of fine sediment storage times, turnover and residual and recently deposited contaminants using the methods presented in this contribution will further aid the implementation of assessment and restoration practices in river basins challenged by siltation, and contemporary and legacy pollution.

4. Conclusions

Fine sediment storage times and the proportion of RDS in the surface of three submerged mid-channel bars in a typical temperate, lowland agricultural river system were estimated using $^{7}Be/^{210}Pb_{ex}$ ratios. Activity ratios varied significantly in time and space reproducing changes in dominant suspended sediment sources, process observations that are globally applicable in other river basin contexts. Sediment storage times and the proportion of RDS were responsive to flood magnitude with two dominant conditions: 1) longer mean storage times and a relatively constant mean proportion of RDS after floods that peaked below 15 $m^3 s^{-1}$, and 2) shorter mean storage times and a significantly higher proportion of RDS after floods that exceeded this river discharge. This finding suggests that fine sediment turnover in these channel bars is dependent on the magnitude of floods, with a limited amount of sediment resuspended during 'normal' high flow events followed by replenishment during the falling limb of the storm hydrograph. It also supports almost complete removal of fines during exceptionally high flow events, with most of it having recently been deposited onto the bars.

Occurrence of both contemporary and legacy particulate contaminants in channel bed sediments were closely related to changes in dominant sediment sources. Naturally occurring and legacy mining trace metals already present in the river system were resuspended during extremely high flow events, significantly increasing their concentrations in the channel sediments. RDC estimations suggest that most of the particulate trace metals were recently deposited onto the bars after the autumn 2022 and winter 2023 floods. RDC estimations for P, on the other hand, were highest in the spring 2022 survey, which is consistent with the seasonal application of phosphate fertiliser to crops.

Fine sediment and associated contaminant and nutrient storage in riverbeds impact habitat quality, as some species benefit from clean and low fine sediment storage substrates with rapid sediment and nutrient

turnover. Longer fine sediment storage times can lead to channel bed colmation or clogging and, with changes in riverine conditions, there is an increased risk for sediment-associated contaminants to become bioavailable, detrimentally impacting river ecology, biodiversity and water quality. Assessment of fine sediment storage times and turnover, and associated contaminant dynamics, using the FRN nuclear tools and techniques demonstrated by this study, will further aid the implementation of mitigation measures in river basins where management strategies set out to tackle the combined global challenge of siltation and sediment-associated pollution.

CRediT authorship contribution statement

Enrique G. Muñoz-Arcos: Writing – original draft, Visualization, Methodology, Investigation, Formal analysis, Data curation, Conceptualization. **Geoffrey E. Millward:** Writing – review & editing, Supervision, Conceptualization. **Caroline C. Clason:** Writing – review & editing, Supervision. **Claudio M. Bravo-Linares:** Writing – review & editing, Supervision. **William H. Blake:** Writing – review & editing, Supervision, Resources, Funding acquisition, Conceptualization.

Funding sources

Funding: This work was supported by the Agencia Nacional de Investigación y Desarrollo (ANID, Chile) [PhD scholarship ID 72210264].

Declaration of competing interest

The authors declare that they have no known competing financial interests or personal relationships that could have appeared to influence the work reported in this paper.

Acknowledgements

E. Munoz-Arcos acknowledges the support of the Agencia Nacional de Investigación y Desarrollo (ANID, Chile) through the PhD scholarship ID 72210264. The work represents a contribution to the joint International Atomic Energy and UN FAO Coordinated Research Programme D1.50.18 “Multiple Isotope Fingerprints to Identify Sources and Transport of Agro-Contaminants”. We are also indebted to landowners Charles Smith, Tom Burner and Adrian Martin for providing sites for river monitoring and access to sampling sites. Richard Hartley, Rupert Goddard, Jess Kitch, Alice Kalnins and Xing Hua are also acknowledged for helping with fieldwork, and Rob Clough for analytical support regarding ICP analysis. The authors thank the reviewers for their valuable comments.

Appendix A. Supplementary data

Supplementary data to this article can be found online at https://doi.org/10.1016/j.scitotenv.2024.178177.

Data availability

The data used in this article is available at Pure system from the University of Plymouth. DOI: 10.24382/791170ce-a3c1-42b0-8464-c3ca81e68a69.

References

Blake, W.H., Walling, D.E., He, Q., 2002. Using cosmogenic beryllium–7 as a tracer in sediment budget investigations. Geogr. Ann. A: Phys. Geogr. 84, 89–102. https://doi.org/10.1111/1468-0459.00163.

Bondarenko, S., Gan, J., 2004. Degradation and sorption of selected organophosphate and carbamate insecticides in urban stream sediments. Environ. Toxicol. Chem. 23, 1809–1814. https://doi.org/10.1897/03-344.

Bonniwell, E.C., Matisoff, G., Whiting, P.J., 1999. Determining the times and distances of particle transit in a mountain stream using fallout radionuclides. Geomorphology 27, 75–92. https://doi.org/10.1016/S0169-555X(98)00091-9.

Bravo-Linares, C., Ovando-Fuentealba, L., Muñoz-Arcos, E., Kitch, J.L., Millward, G.E., López-Gajardo, R., Cañoles-Zambrano, M., Del Valle, A., Kelly, C., Blake, W.H., 2024. Basin scale sources of siltation in a contaminated hydropower reservoir. Sci. Total Environ. 914, 169952. https://doi.org/10.1016/j.scitotenv.2024.169952.

Bylak, A., Kukuła, K., 2022. Impact of fine-grained sediment on mountain stream macroinvertebrate communities: forestry activities and beaver-induced sediment management. Sci. Total Environ. 832, 155079. https://doi.org/10.1016/j.scitotenv.2022.155079.

Collins, A.L., Walling, D.E., 2007. Fine-grained bed sediment storage within the main channel systems of the Frome and Piddle catchments, Dorset, UK. Hydrol. Process. 21, 1448–1459. https://doi.org/10.1002/hyp.6269.

Cornett, R.J., Chant, L.A., Risto, B.A., Bonvin, E., 1994. Identifying resuspended particles using isotope ratios. Hydrobiologia 284, 69–77. https://doi.org/10.1007/BF00005732.

Dines, H.G., 1956, 1891- The Metalliferous Mining Region of South-West England, Memoirs of the Geological Survey of Great Britain. H.M. Stationery Office, London.

Dong, J., Xia, X., Zhai, Y., 2013. Investigating particle concentration effects of polycyclic aromatic hydrocarbon (PAH) sorption on sediment considering the freely dissolved concentrations of PAHs. J. Soil. Sediment. 13, 1469–1477. https://doi.org/10.1007/s11368-013-0736-9.

Downs, P.W., Soar, P.J., Taylor, A., 2016. The anatomy of effective discharge: the dynamics of coarse sediment transport revealed using continuous bedload monitoring in a gravel-bed river during a very wet year. Earth Surf. Process. Landf. 41, 147–161. https://doi.org/10.1002/esp.3785.

Du Laing, G., Rinklebe, J., Vandecasteele, B., Meers, E., Tack, F.M.G., 2009. Trace metal behaviour in estuarine and riverine floodplain soils and sediments: a review. Sci. Total Environ. 407, 3972–3985. https://doi.org/10.1016/j.scitotenv.2008.07.025.

Du, J.Z., Zhang, J., Baskaran, M., 2011. Applications of short-lived radionuclides (7Be, 210Pb, 210Po, 137Cs and 234Th) to trace the sources, transport pathways, and deposition of particles/sediments in rivers, estuaries and coasts. Handbook of Environmental Isotope Geochemistry 305–329.

Dubuis, R., De Cesare, G., 2023. The clogging of riverbeds: a review of the physical processes. Earth Sci. Rev. 239, 104374. https://doi.org/10.1016/j.earscirev.2023.104374.

Evans, E., Wilcox, A.C., 2014. Fine sediment infiltration dynamics in a gravel-bed river following a sediment pulse. River Res. Appl. 30, 372–384. https://doi.org/10.1002/rra.2647.

Evrard, O., Laceby, J.P., Huon, S., Lefèvre, I., Sengtaheuanghoung, O., Ribolzi, O., 2016. Combining multiple fallout radionuclides (^{137}Cs, ^{7}Be, ^{210}Pbxs) to investigate temporal sediment source dynamics in tropical, ephemeral riverine systems. J. Soil. Sediment. 16, 1130–1144. https://doi.org/10.1007/s11368-015-1316-y.

Fisher, G.B., Magilligan, F.J., Kaste, J.M., Nislow, K.H., 2010. Constraining the timescales of sediment sequestration associated with large woody debris using cosmogenic ^{7}Be. J. Geophys. Res. Earth Surf. 115. https://doi.org/10.1029/2009JF001352.

Frings, R.M., Ten Brinke, W.B.M., 2018. Ten reasons to set up sediment budgets for river management. Int. J. River Basin Manag. 16, 35–40. https://doi.org/10.1080/15715124.2017.1345916.

Froger, C., Ayrault, S., Gasperi, J., Caupos, E., Monvoisin, G., Evrard, O., Quantin, C., 2019. Innovative combination of tracing methods to differentiate between legacy and contemporary PAH sources in the atmosphere-soil-river continuum in an urban catchment (Orge River, France). Sci. Total Environ. 669, 448–458. https://doi.org/10.1016/j.scitotenv.2019.03.150.

Fryirs, K., 2013. (dis)connectivity in catchment sediment cascades: a fresh look at the sediment delivery problem. Earth Surf. Process. Landf. 38, 30–46. https://doi.org/10.1002/esp.3242.

Gartner, J.D., Renshaw, C.E., Dade, W.B., Magilligan, F.J., 2012. Time and depth scales of fine sediment delivery into gravel stream beds: constraints from fallout radionuclides on fine sediment residence time and delivery. Geomorphology 151, 39–49. https://doi.org/10.1016/j.geomorph.2012.01.008.

Gellis, A.C., Fuller, C.C., Van Metre, P.C., 2017. Sources and ages of fine-grained sediment to streams using fallout radionuclides in the Midwestern United States. J. Environ. Manage. 194, 73–85. https://doi.org/10.1016/j.jenvman.2016.06.018.

Gellis, A.C., Fuller, C.C., Van Metre, P., Filstrup, C.T., Tomer, M.D., Cole, K.J., Sabitov, T.Y., 2019. Combining sediment fingerprinting with age-dating sediment using fallout radionuclides for an agricultural stream, Walnut Creek, Iowa, USA. J. Soil. Sediment. 19, 3374–3396. https://doi.org/10.1007/s11368-018-2168-z.

Gerolin, C.R., Pupim, F.N., Sawakuchi, A.O., Grohmann, C.H., Labuto, G., Semensatto, D., 2020. Microplastics in sediments from Amazon rivers, Brazil. Sci. Total Environ. 749, 141604. https://doi.org/10.1016/j.scitotenv.2020.141604.

Gourdin, E., Evrard, O., Huon, S., Reyss, J.-L., Ribolzi, O., Bariac, T., Sengtaheuanghoung, O., Ayrault, S., 2014. Spatial and temporal variability of ^{7}Be and ^{210}Pb wet deposition during four successive monsoon storms in a catchment of northern Laos. J. Environ. Radioact. 136, 195–205. https://doi.org/10.1016/j.jenvrad.2014.06.008.

Gurnell, A.M., Bertoldi, W., 2022. The impact of plants on fine sediment storage within the active channels of gravel-bed rivers: a preliminary assessment. Hydrol. Process. 36, e14637. https://doi.org/10.1002/hyp.14637.

Hancock, G.J., Wilkinson, S.N., Hawdon, A.A., Keen, R.J., 2014. Use of fallout tracers ^{7}Be, ^{210}Pb and ^{137}Cs to distinguish the form of sub-surface soil erosion delivering sediment to rivers in large catchments. Hydrol. Process. 28, 3855–3874. https://doi.org/10.1002/hyp.9926.

Hawley, N., Robbins, J.A., Eadie, B.J., 1986. The partitioning of ^{7}beryllium in fresh water. Geochim. Cosmochim. Acta 50, 1127–1131. https://doi.org/10.1016/0016-7037(86)90393-5.

Hurley, R., Woodward, J., Rothwell, J.J., 2018. Microplastic contamination of river beds significantly reduced by catchment-wide flooding. Nat. Geosci. 11, 251–257. https://doi.org/10.1038/s41561-018-0080-1.

Jones, J.I., Murphy, J.F., Collins, A.L., Sear, D.A., Naden, P.S., Armitage, P.D., 2012. The impact of fine sediment on macro-invertebrates. River Res. Appl. 28, 1055–1071. https://doi.org/10.1002/rra.1516.

Jweda, J., Baskaran, M., van Hees, E., Schweitzer, L., 2008. Short-lived radionuclides (^{7}Be and ^{210}Pb) as tracers of particle dynamics in a river system in Southeast Michigan. Limnol. Oceanogr. 53, 1934–1944. https://doi.org/10.4319/lo.2008.53.5.1934.

Karwan, D.L., Pizzuto, J.E., Aalto, R., Marquard, J., Harpold, A., Skalak, K., Benthem, A., Levia, D.F., Siegert, C.M., Aufdenkampe, A.K., 2018. Direct channel precipitation and storm characteristics influence short-term fallout radionuclide assessment of sediment source. Water Resour. Res. 54, 4579–4594. https://doi.org/10.1029/2017WR021684.

Kaste, J.M., Baskaran, M., 2011. Meteoric ^{7}Be and ^{10}Be as process tracers in the environment. Handbook of Environmental Isotope Geochemistry 61–85.

Kaste, J.M., Norton, S.A., Hess, C.T., 2002. Environmental chemistry of beryllium-7. Rev. Mineral. Geochem. 50, 271–289. https://doi.org/10.2138/rmg.2002.50.6.

Kaste, J.M., Magilligan, F.J., Renshaw, C.E., Burch Fisher, G., Brian Dade, W., 2014. Seasonal controls on meteoric ^{7}Be in coarse-grained river channels. Hydrol. Process. 28, 2738–2748. https://doi.org/10.1002/hyp.9800.

Kemp, P., Sear, D., Collins, A., Naden, P., Jones, I., 2011. The impacts of fine sediment on riverine fish. Hydrol. Process. 25, 1800–1821. https://doi.org/10.1002/hyp.7940.

Lambert, C.P., Walling, D.E., 1988. Measurement of channel storage of suspended sediment in a gravel-bed river. Catena 15, 65–80. https://doi.org/10.1016/0341-8162(88)90017-3.

Le Gall, M., Evrard, O., Foucher, A., Laceby, J.P., Salvador-Blanes, S., Maniere, L., Lefevre, I., Cerdan, O., Ayrault, S., 2017. Investigating the temporal dynamics of suspended sediment during flood events with Be-7 and Pb-210(xs) measurements in a drained lowland catchment. Sci. Rep. 7, 42099. https://doi.org/10.1038/srep42099.

Lee, B.J., Kim, J., Hur, J., Choi, I.H., Toorman, E.A., Fettweis, M., Choi, J.W., 2019. Seasonal dynamics of organic matter composition and its effects on suspended sediment flocculation in river water. Water Resour. Res. 55, 6968–6985. https://doi.org/10.1029/2018WR024486.

Marttila, H., Kløve, B., 2014. Storage, properties and seasonal variations in fine-grained bed sediment within the main channel and headwaters of the River Sanginjoki, Finland. Hydrol. Process. 28, 4756–4765. https://doi.org/10.1002/hyp.9953.

Matisoff, G., 2014. ^{210}Pb as a tracer of soil erosion, sediment source area identification and particle transport in the terrestrial environment. J. Environ. Radioact. 138, 343–354. https://doi.org/10.1016/j.jenvrad.2014.03.008.

Matisoff, G., Wilson, C.G., Whiting, P.J., 2005. The Be-7/Pb-210(xs) ratio as an indicator of suspended sediment age or fraction new sediment in suspension. Earth Surf. Process. Landf. 30, 1191–1201. https://doi.org/10.1002/esp.1270.

Millward, G.E., Blake, W.H., 2023. Distribution and storage of uranium, and its decay products, in floodplain sediments. Environ. Pollut. 324, 121356. https://doi.org/10.1016/j.envpol.2023.121356.

Muñoz-Arcos, E., Millward, G.E., Clason, C.C., Bravo-Linares, C., Blake, W.H., 2022. Understanding the complexity of sediment residence time in rivers: application of fallout radionuclides (FRNs). Earth Sci. Rev. 233, 104188. https://doi.org/10.1016/j.earscirev.2022.104188.

Muñoz-Arcos, E., Millward, G.E., Clason, C.C., Hartley, R., Bravo-Linares, C., Blake, W.H., 2024. Variability of fallout radionuclides (FRNs) in river channels: implications for sediment tracing. J. Soil. Sediment. https://doi.org/10.1007/s11368-024-03881-z.

Naden, P.S., Murphy, J.F., Old, G.H., Newman, J., Scarlett, P., Harman, M., Duerdoth, C.P., Hawczak, A., Pretty, J.L., Arnold, A., Laizé, C., Hornby, D.D., Collins, A.L., Sear, D.A., Jones, J.I., 2016. Understanding the controls on deposited fine sediment in the streams of agricultural catchments. Sci. Total Environ. 547, 366–381. https://doi.org/10.1016/j.scitotenv.2015.12.079.

Olsen, C.R., Larsen, I.L., Lowry, P.D., Cutshall, N.H., Nichols, M.M., 1986. Geochemistry and deposition of 7Be in river-estuarine and coastal waters. J. Geophys. Res. Oceans 91, 896–908. https://doi.org/10.1029/JC091iC01p00896.

Olsen, C.R., Thein, M., Larsen, I.L., Lowry, P.D., Mulholland, P.J., Cutshall, N.H., Byrd, J.T., Windom, H.L., 1989. Plutonium, lead-210, and carbon isotopes in the Savannah estuary: riverborne versus marine sources. Environ. Sci. Technol. 23, 1475–1481. https://doi.org/10.1021/es00070a004.

Owens, P.N., 2020. Soil erosion and sediment dynamics in the Anthropocene: a review of human impacts during a period of rapid global environmental change. J. Soil. Sediment. 20, 4115–4143. https://doi.org/10.1007/s11368-020-02815-9.

Owens, P.N., Batalla, R.J., Collins, A.J., Gomez, B., Hicks, D.M., Horowitz, A.J., Kondolf, G.M., Marden, M., Page, M.J., Peacock, D.H., Petticrew, E.L., Salomons, W., Trustrum, N.A., 2005. Fine-grained sediment in river systems: environmental significance and management issues. River Res. Appl. 21, 693–717. https://doi.org/10.1002/rra.878.

Phillips, J.M., Russell, M.A., Walling, D.E., 2000. Time-integrated sampling of fluvial suspended sediment: a simple methodology for small catchments. Hydrol. Process. 14, 2589–2602. https://doi.org/10.1002/1099-1085(20001015)14:14<2589::AID-HYP94>3.3.CO;2-4.

Pulley, S., Goubet, A., Moser, I., Browning, S., Collins, A.L., 2019. The sources and dynamics of fine-grained sediment degrading the Freshwater Pearl Mussel (Margaritifera margaritifera) beds of the River Torridge, Devon, UK. Sci. Total Environ. 657, 420–434. https://doi.org/10.1016/j.scitotenv.2018.11.401.

Skalak, K., Pizzuto, J., 2010. The distribution and residence time of suspended sediment stored within the channel margins of a gravel-bed bedrock river. Earth Surf. Process. Landf. 35, 435–446. https://doi.org/10.1002/esp.1926.

Svendsen, K.M., Renshaw, C.E., Magilligan, F.J., Nislow, K.H., Kaste, J.M., 2009. Flow and sediment regimes at tributary junctions on a regulated river: impact on sediment residence time and benthic macroinvertebrate communities. Hydrol. Process. 23, 284–296. https://doi.org/10.1002/hyp.7144.

Van Hoof, P.L., Andren, A.W., 1989. Partitioning and transport of ^{210}Pb in Lake Michigan. J. Great Lakes Res. 15, 498–509. https://doi.org/10.1016/S0380-1330(89)71505-7.

Van Metre, P.C., Mahler, B.J., Qi, S.L., Gellis, A.C., Fuller, C.C., Schmidt, T.S., 2022. Sediment sources and sealed-pavement area drive polycyclic aromatic hydrocarbon and metal occurrence in urban streams. Environ. Sci. Technol. 56, 1615–1626. https://doi.org/10.1021/acs.est.1c00414.

Walling, D.E., 1983. The sediment delivery problem. J. Hydrol. 65, 209–237. https://doi.org/10.1016/0022-1694(83)90217-2.

Walling, D.E., 2013. Beryllium-7: the cinderella of fallout radionuclide sediment tracers? Hydrol. Process. 27, 830–844. https://doi.org/10.1002/hyp.9546.

Walling, D.E., Woodward, J.C., 1992. Use of radiometric fingerprints to derive information on suspended sediment sources. In: Bolen, J. (Ed.), Erosion and Sediment Monitoring Programmes in River Basins. Proc. International Symposium, Oslo, 1992|. International Association of Hydrological Sciences, pp. 153–164.

Wang, X., Blake, W.H., Taylor, A., Kitch, J., Millward, G., 2021. Evaluating the effectiveness of soil conservation at the basin scale using floodplain sedimentary archives. Sci. Total Environ. 792, 148414. https://doi.org/10.1016/j.scitotenv.2021.148414.

Wharton, G., Mohajeri, S.H., Righetti, M., 2017. The pernicious problem of streambed colmation: a multi-disciplinary reflection on the mechanisms, causes, impacts, and management challenges. Wiley Interdiscip. Rev.: Water 4, e1231. https://doi.org/10.1002/wat2.1231.

Wilkes, M.A., Gittins, J.R., Mathers, K.L., Mason, R., Casas-Mulet, R., Vanzo, D., Mckenzie, M., Murray-Bligh, J., England, J., Gurnell, A., Jones, J.I., 2019. Physical and biological controls on fine sediment transport and storage in rivers. Wiley Interdiscip. Rev.: Water 6, e1331. https://doi.org/10.1002/wat2.1331.

Wohl, E., 2015. Legacy effects on sediments in river corridors. Earth Sci. Rev. 147, 30–53. https://doi.org/10.1016/j.earscirev.2015.05.001.

Wohl, E., 2021. An integrative conceptualization of floodplain storage. Rev. Geophys. 59, e2020RG000724. https://doi.org/10.1029/2020RG000724.